

ARTICLE



Frequency-specific and state-dependent neural responses to brain stimulation

Huichun Luo^{1,2,3,11}, Xiaolai Ye^{1,4,5,11}, Hui-Ting Cai^{1,2,6,11}, Mo Wang^{7,11}, Yue Wang⁷, Qiangqiang Liu^{1,4}, Ying Xu², Ziyu Mao⁴, Yanqing Cai⁴, Jing Hong⁴, Chencheng Zhang⁸, Pengfei Wei^{1,9}, Yong Lu¹⁰, Quanying Liu^{1,7}, Jiwen Xu^{1,4} and Ti-Fei Yuan^{1,2,3}✉

© The Author(s), under exclusive licence to Springer Nature Limited 2025

Non-invasive brain stimulation is promising for treating many neuropsychiatric and neurological conditions. It could be optimized by understanding its intracranial responses in different brain regions. We implanted multi-site intracranial electrodes and systematically assessed the acute responses in these regions to transcranial alternating current stimulation (tACS) at different frequencies. We observed robust neural oscillation changes in the hippocampus and amygdala in response to non-invasive tACS procedures, and these effects were frequency-specific and state-dependent. Notably, the hippocampus responded most strongly and stably to 10 Hz stimulation, with pronounced changes across a wide frequency range, suggesting the potential of 10 Hz oscillatory stimulation to modulate a broad range of neural activity related to cognitive functions. Future work with increased sample sizes is required to determine the clinical implications of these findings for therapeutic efficiency.

Molecular Psychiatry; <https://doi.org/10.1038/s41380-025-02892-7>

INTRODUCTION

Modulating brain rhythms, such as with transcranial alternating current stimulation (tACS), provides an important, non-invasive, and non-pharmacological approach to manipulating brain function in both physiological and diseased states [1, 2]. Phase-locking of intrinsic brain rhythms (e.g., that of the hippocampus) through frequency-specific modulation or cross-frequency coupling could help improve both working and long-term memory [3–5]. Notably, chronic gamma band tACS over the temporal lobe or the precuneus improves cognition in Alzheimer's disease patients, potentially through its effects on recruiting memory processing-related networks (e.g., via hippocampal-cortical network) [6–8]. Though there is clear evidence that tACS may serve as a neural oscillatory tuning procedure with frequency precision, the frequency-sensitive responses of the live human brain, which may act as an active signal filter, remain largely unknown in this therapeutic context, which limits our current ability to optimize the clinical use of tACS for specific conditions [9–12].

Based on entrainment theory, an external alternating electrical field could drive temporal alignment of neuronal activity and facilitate cross-regional synchronization of neural oscillations. Non-human primate studies have indicated that prefrontal tACS could

align the spike timing of certain hippocampal neurons to the external stimulation phase in a frequency-specific manner [3]. There is further evidence for a dose-dependent response pattern, such that the spike entrainment in responsive neurons gradually increases following higher tACS intensity [13]. On the other hand, the Arnold tongue theory proposes that the brain functions as an active signal filter and tends to respond to external frequencies adjacent to the intrinsic oscillation or its harmonic, resulting in the enhancement of the intrinsic oscillations [14–16]. Evidence for this has been presented based on the dominant alpha oscillations of awake ferrets and human brains [14, 15]. The tACS frequencies matched to the intrinsic alpha peak exhibit enhanced coupling between neuronal spiking and tACS, regardless of stimulation intensity. In contrast, tACS frequencies different from intrinsic alpha require higher stimulation intensities to achieve similar coupling enhancement [14]. As a result, a dual modulatory pattern emerges: tACS first recruits brain regions with intrinsic oscillation frequencies close to the external stimulation frequency, then expands to other regions when the stimulation intensity is gradually increased [16]. However, this model neglects the involvement of endogenous oscillations of brain regions, and also the fact that the brain state is maintained through large-scale

¹Department of Neurosurgery, Clinical Neuroscience Center Comprehensive Epilepsy Unit, Ruijin Hospital Luwan Branch, Shanghai Jiao Tong University School of Medicine, Shanghai, China. ²Shanghai Key Laboratory of Psychotic Disorders, Brain Health Institute, National Center for Mental Disorders, Shanghai Mental Health Center, Shanghai Jiao Tong University School of Medicine and School of Psychology, Shanghai, China. ³Co-innovation Center of Neuroregeneration, Nantong University, Nantong, China. ⁴Department of Neurosurgery, Clinical Neuroscience Center Comprehensive Epilepsy Unit, Ruijin Hospital, Shanghai Jiao Tong University School of Medicine, Shanghai, China. ⁵Department of Neurology, Shanghai Children's Medical Center, School of Medicine, Shanghai Jiao Tong University, Shanghai, China. ⁶Shanghai Xuhui Mental Health Center, Shanghai, China. ⁷Shenzhen Key Laboratory of Smart Healthcare Engineering, Southern University of Science and Technology, Shenzhen, China. ⁸Department of Neurosurgery, Center for Functional Neurosurgery, Ruijin Hospital, Shanghai Jiao Tong University School of Medicine, Shanghai, China. ⁹Shenzhen Key Laboratory of Neuropsychiatric Modulation and Collaborative Innovation Center for Brain Science, Guangdong Provincial Key Laboratory of Brain Connectome and Behavior, CAS Center for Excellence in Brain Science and Intelligence Technology, Brain Cognition and Brain Disease Institute, Shenzhen Institute of Advanced Technology, Chinese Academy of Sciences, Shenzhen-Hong Kong Institute of Brain Science, Shenzhen Fundamental Research Institutions, Shenzhen, China. ¹⁰Department of Radiology, Ruijin Hospital, Shanghai Jiao Tong University School of Medicine, Shanghai, China. ¹¹These authors contributed equally: Huichun Luo, Xiaolai Ye, Hui-Ting Cai, Mo Wang. ✉email: liuyq@sustech.edu.cn; xjw88@vip.163.com; ytf0707@126.com

Received: 18 April 2024 Revised: 10 December 2024 Accepted: 10 January 2025

Published online: 20 January 2025

network-level interactions among many brain regions [17]. For instance, one study reported that low-frequency (0.75 Hz or 1 Hz) tACS over the frontal and occipital poles failed to enhance the intrinsic slow oscillations (~1 Hz) that dominate during non-rapid eye movement sleep [18]. Therefore, it is critical to obtain intracranial neurophysiological signals before and after non-invasive brain stimulation in order to understand the potential competition and synergy between exogenous and endogenous electrical fields.

In the present study, we implanted multi-site intracranial electrodes to record local field potentials (LFPs) of the hippocampus and amygdala in response to tACS procedures at different frequencies. The tACS procedures focused on two montages (F3-Fp2 and F4-Fp1) over the prefrontal cortex, which have been shown to significantly improve cognitive performance in healthy people [19] and are also commonly employed in clinical treatment for psychiatric disorders such as depression as well as cognitive disorders [20]. The hippocampus and amygdala are closely associated with cognitive functions linked to psychiatric disorders, such as emotion [21, 22] and memory [23]. Most importantly, a recent study revealed that these regions are crucial in understanding the effects of neuromodulation over the prefrontal cortex [24]. Therefore, in the present study we mainly focused on the neural oscillation activity of the hippocampus and amygdala. We first analyzed the LFPs before, during, and after tACS to capture the immediate and lasting effect of tACS on neural oscillations. We then calculated the correlation between the effect of tACS on neural oscillations and the pre-stimulation level of endogenous neural oscillations to reveal whether there is a dependency relationship between them. The results of this study provide support for the notion that human brain oscillations function as an active signal filter, in that oscillations of deep brain regions respond strongly to specific frequencies and the strength of the response depends partly on the innate oscillation activity level. In particular, we found robust neural oscillation changes in the hippocampus under 10 Hz tACS. These findings provide evidence for frequency-specific and state-dependent responses in the live human brain and suggest that 10 Hz tACS may have stronger effects than other frequencies.

MATERIALS AND METHODS

Participants

Data were obtained from epileptic patients undergoing stereo electroencephalogram (SEEG) to localize epileptic foci for potential surgical resection at the Ruijin Hospital Luwan Branch, Shanghai Jiao Tong University, Shanghai, China, Epilepsy Center. Intracranial depth electrodes (5–20 contacts, 0.8 mm diameter, 2 mm each contact, 1.5 mm spacing, Huake Hengsheng, Beijing, China or Alcis, Besancon, France) were stereotactically implanted with a stereotactic robot system (Sinovation, Huake, China). Clinical needs exclusively guided the electrode placements. All procedures performed in studies involving human participants strictly followed the ethical standards of the institutional research committee, the 1964 Helsinki Declaration and its later amendments, or comparable ethical standards. The ethics committee of Ruijin Hospital, Shanghai Jiao Tong University School of Medicine, approved all procedures used. All patients provided written informed consent following the Declaration of Helsinki.

Sex as a biological variable

Our study included 2 male and 6 female participants. Sex was not considered as a biological variable.

Electrode localization

Electrodes were localized in each participant using co-registered pre-implantation T1-weighted MRI and post-implantation CT images transformed into MNI ICBM152 coordinates using affine co-registration in Brainstorm toolbox (<https://neuroimage.usc.edu/brainstorm>). Intracranial electrodes were reconstructed by identifying the tip and trajectory of each electrode shaft. For the hippocampus and amygdala, the reconstruction

was overlayed on the subcortical ASEG atlas to verify which contacts were located within regions of interest [25].

Experimental design

In epileptic patients undergoing SEEG monitoring, it is feasible to record LFPs from deep brain regions while giving tACS. We administered tACS at four different frequencies (5 Hz, 10 Hz, 20 Hz, and 40 Hz) to each patient, with each frequency of stimulation administered twice in a random order. A typical trial began with a 120 s pre-stimulation rest period, ~90 s of stimulation including 20 s ramp-up +70 s full intensity stimulation +2 s ramp down, and a 120 s post-stimulation rest period. Patients were asked to rest with their eyes closed during the resting periods. The interval between trials was 5 min. Each participant received only one type of tACS montage (F3-Fp2 or F4-Fp1 montage (10–20 system)), with the location of the montage determined based on the location of scalp damage from SEEG electrode implantation, ensuring that the stimulating electrodes were at least 5 cm away from the scalp damage caused by SEEG electrode implantation. Bipolar alternating current stimulations were performed at 2 mA intensity, except for Sub001, for whom the stimulation intensity was reduced to 1.5 mA due to intolerance.

Data acquisition

LFPs were acquired using a Nihon Kohden recording system (256 channel amplifier, model JE120A), analog-filtered above 0.01 Hz, and digitally sampled at 2000 Hz. tACS was performed using two circular electrodes (3.5 cm external diameter). Both were inserted in a square electrode holder (4 cm length) filled with physiological saline, creating a 12.25 cm² stimulation area on the scalp for each electrode. The impedance was checked before, during, and after each stimulation to ensure the patient did not experience an obvious pain sensation. The stimulation was delivered through these electrodes using a TES stimulator (Fo.cus V3, London, UK). This device is widely used in clinical and scientific research [26–28]. Moreover, we have demonstrated that the device can stably output specified stimulation under different parameters and environments through systematic testing (See Appendix 1. "Stimulation Device Investigation" in the Supplementary Material). Participants reported no side effects during the study except for mild skin sensations (tickling).

Simulated electric field calculation

We utilized the SimNIBS 2.1 package to perform finite element method (FEM) simulations [29]. To create individualized models, we used CHARM, a pipeline built into SimNIBS, to process personalized T1-weighted images and generate FEM models [30]. The input images were first segmented into brain tissues, which were then converted into meshes. Each mesh was assigned a conductivity value corresponding to the tissue type. For our experiments, we used the default conductivity settings: White Matter (0.126 S/m), Gray Matter (0.275 S/m), CSF (1.654 S/m), Compact Bone (0.008 S/m), Spongy Bone (0.025 S/m), Scalp (0.465 S/m), and Eyeballs (0.5 S/m). The FEM model assumes that there are no internal activities within the brain, meaning no net current sources or sinks exist within the elements. Thus, the electric field (EF) of each mesh can be calculated using the following Poisson equation:

$$\nabla \cdot (\sigma E) = -\nabla \cdot (\sigma \nabla V) = 0 \quad (1)$$

where E is the electric field, σ is the tissue conductivity, and V is the potential distribution. Then, we used the FEM to assemble them into a globe matrix and defined the boundary conditions based on electrode settings. Electrode locations were determined based on experimental setups and calculated using a built-in morphological approach. During stimulation, we applied 2 mA to each electrode. Utilizing the potential from the electrodes (V_0), which is determined by factors such as the electrode material, size, and placement, we can apply the Dirichlet boundary condition:

$$V = V_0 \quad (2)$$

After assembling the global matrix and applying the boundary conditions, the system was solved numerically to obtain the distribution in the EF of a single direction. The average EF norm was calculated from the three orthogonal field components using Eq. (3):

$$E = \sqrt{E_x^2 + E_y^2 + E_z^2} \quad (3)$$

where x, y, and z represent three orthogonal directions.

Finally, to compare EFs between subjects, the locations of individual contact were non-linear and transformed to MNI space. The EF distributions simulated during peak current were extracted and displayed on a surface view. A perspective version allowed us to see EF intensity distribution in the hippocampus and amygdala.

Real electric field calculation based on LFP

The real EF was obtained by calculating the gradient of the voltage measured on each contact of the same SEEG electrode. Specifically, the procedure included four steps: (a) An 8 s segment of the raw LFP (monopolar signal) during full-intensity stimulation and without visible artifacts was selected for calculating the EF. (b) A baseline correction was performed on the selected segment signal to avoid potential DC offset and artifacts by subtracting the mean of a 2 s window right before the stimulation. (c) A fast Fourier transform (FFT) was applied to the signal and the two-sided power spectrum was converted to a single-sided power spectrum. The number of points at which the FFT was performed (nfft) is 2048. Then, the absolute value of the single-sided power spectrum was normalized by dividing nfft/2 (nfft for 0 Hz), yielding the amplitude of each frequency point. The amplitude of stimulation was taken to be the maximum value around ± 2 Hz of stimulation frequency. (d) Finally, the stimulation amplitudes of contacts in the same electrode were used to calculate the gradient, and this calculation was repeated for all SEEG electrodes.

The gradient calculated the central difference for interior data points. For example, consider an electrode with unit-spaced, voltage of contact A_i , that has a horizontal gradient $G = \text{gradient}(A)$. The interior gradient values, G_i , are:

$$G_i = 0.5 * (A_{i+1} - A_{i-1}) \quad (4)$$

Where i varies between 2 and N-1, and N is the number of contacts of the electrode.

The gradient values of the contact at the edges of the electrode are calculated with single-sided differences so that

$$G_1 = A_2 - A_1 \quad (5)$$

$$G_N = A_N - A_{N-1} \quad (6)$$

We tested this algorithm on a simulated sine wave signal and proved it could calculate the actual peak amplitude of a sine wave (See Appendix 2. "Algorithm of Peak Amplitude Calculating" in the Supplementary Material). It should be noted that to calculate the actual EF, the voltage gradient needs to be divided by the distance between the contacts, which was 3.5 mm in this study.

Signal preprocessing

The raw LFPs were first divided into pre-stimulation, during-stimulation (only full-intensity part 70 s), and post-stimulation segments. The steps for LFP data preprocessing were as follows: (a) Each electrode was converted to bipolar by differentiating the signals of two adjacent contacts on the electrodes. (b) Low-pass filtering was performed at 200 Hz with a Chebyshev Type I filter to rule out LFP oscillatory activities not of interest. (c) High-pass filtering was performed at 1 Hz with a Chebyshev Type I filter to eliminate baseline shifting. (d) Sinusoid removal was performed (only for during-stimulation segments). This process eliminates stimulus artifacts by identifying the sinusoidal components and subtracting them from the signals in the same time domain (Supplementary Fig. 1). (e) Data was down-sampled to 1000 Hz to reduce storage space and enhance computational efficiency. (f) The continuous data was segmented into non-overlapping, fixed 2-second time windows. Then, two epileptologists (XLY and LHC) visually screened all epochs separately to identify and remove epileptiform discharges and other artifacts that appeared intermittently. To reduce potential bias, only epochs that both epileptologists agreed were free of artifacts were included in further analysis. The surviving epoch rate was defined as the proportion of epochs available for analysis relative to the total number of epochs recorded in each trial.

Subsequently, the preprocessed segmented LFP data between 1 and 200 Hz were decomposed into seven different frequency-band oscillations: delta (δ , 1–4 Hz), theta (θ , 4–8 Hz), alpha (α , 8–12 Hz), beta (β , 12–30 Hz), low-gamma (γ_L , 30–60 Hz), high-gamma (γ_H , 60–90 Hz), and ultra-frequency

(u, 90–200 Hz). The analysis of the LFP data was performed offline with custom-developed scripts in MATLAB (MathWorks Inc., Natick, MA, USA).

Power change ratio calculation

The power spectra density (PSD) of each epoch was calculated using a FFT with a 2 s sliding window and a 1 s overlap. To reduce the influence of inter-individual variability, the PSD was normalized by dividing the values by the integral power between 1 and 200 Hz. Finally, for each channel, the normalized PSD values of all epochs were averaged, and the power of each oscillation was the area under the curve within its frequency range. Next, we calculated the power change ratios of during- and post-stimulation relative to the baseline to represent the neural oscillations induced by tACS. The power change ratio was calculated as follows: (PSD of during-stimulation or PSD of post-stimulation minus PSD of pre-stimulation) divided by the PSD of pre-stimulation, multiplied by 100%.

Analyzing the effect of tACS on oscillations

To check for an overall change during- and post-stimulation, we initially combined the data under all the stimulating montages and frequencies, then used a threshold of 5% change rate to categorize the neural oscillations induced by tACS into three response types: facilitated (power change ratio $>5\%$), inhibited (power change ratio $<-5\%$), and no response (power change ratio within $[-5\% \text{ to } 5\%]$). We assessed whether the distribution of different response types differed between during- and post-stimulation using Chi-square tests on data from the hippocampus and amygdala. Additionally, we also examined other thresholds (10, 20, 30, and 40%) to ensure the reproducibility of the results.

To identify the specific effect of tACS at different frequencies on neural oscillations, we first divided the participants into two groups according to the relative locations of the recording and stimulating electrodes to control the confounding factor related to the position of the stimulating electrodes. Subsequently, statistical analysis was performed individually to evaluate the neural response of each frequency band at each stimulation frequency in each group. For each statistical test, the distribution of the data was examined first to help choose the appropriate statistical method. If the data conformed to the normal distribution (Shapiro-Wilks normality test), a one-sample t-test was performed; otherwise, the Wilcoxon signed-rank test was used. Here, the null hypothesis was that tACS did not affect neural oscillations, whereas the alternative hypothesis was that tACS significantly affected neural oscillations.

State-dependent analysis

To investigate the relationship between the effect of tACS and the original brain state of participants, we further calculated the correlation between the PSD of pre-stimulation and the power change ratio of during- or post-stimulation. The Spearman test was applied to evaluate each correlation since most data did not conform to the normal distribution. For all statistical tests, the significance levels were set to $p < 0.01$, and all reported p-values were corrected for multiple comparisons using the FDR correction.

RESULTS

In total, eight epileptic patients (six females, two males, age range 16–48; more information is included in Table 1) with electrodes in the amygdala or the head of the hippocampus participated. All participants were right-handed, did not evidence cognitive impairment (MoCA score >20), and had no neurological or psychiatric disorders other than epilepsy. Participants were off medication for at least 12 h at the time of testing. Participants were seizure-free for 12 h before and during the test. As shown in Fig. 1b, there were 6 electrodes in the head of the hippocampus (one electrode was excluded since it was in the seizure zone, so we ultimately analyzed 16 channels of bipolar recordings from 21 contacts in 5 electrodes) and 8 electrodes in the amygdala (25 channels of bipolar recording from 33 contacts).

Electric field distribution

This study focused on two montages (F3-Fp2 and F4-Fp1) over the prefrontal cortex (as shown in Fig. 1a). We first calculated the EF

Table 1. Patient demographics.

| No. | Gender | Age (year) | Education (year) | Diagnosed epileptogenic zone | Handedness | MOCA |
|--------|--------|------------|------------------|------------------------------|------------|------|
| Sub001 | Male | 16 | 9 | L Inferior Temporal | Right | 20 |
| Sub002 | Female | 32 | 15 | R Operculum | Right | 28 |
| Sub003 | Male | 25 | 16 | L Hippocampus | Right | 21 |
| Sub004 | Female | 19 | 12 | L Middle-posterior Temporal | Right | 24 |
| Sub005 | Female | 48 | 9 | R Hippocampus | Right | 20 |
| Sub006 | Female | 30 | 12 | R Prefrontal | Right | 24 |
| Sub007 | Female | 19 | 15 | R Rolandic | Right | 26 |
| Sub008 | Female | 23 | 16 | L Parietooccipital sulcus | Right | 27 |

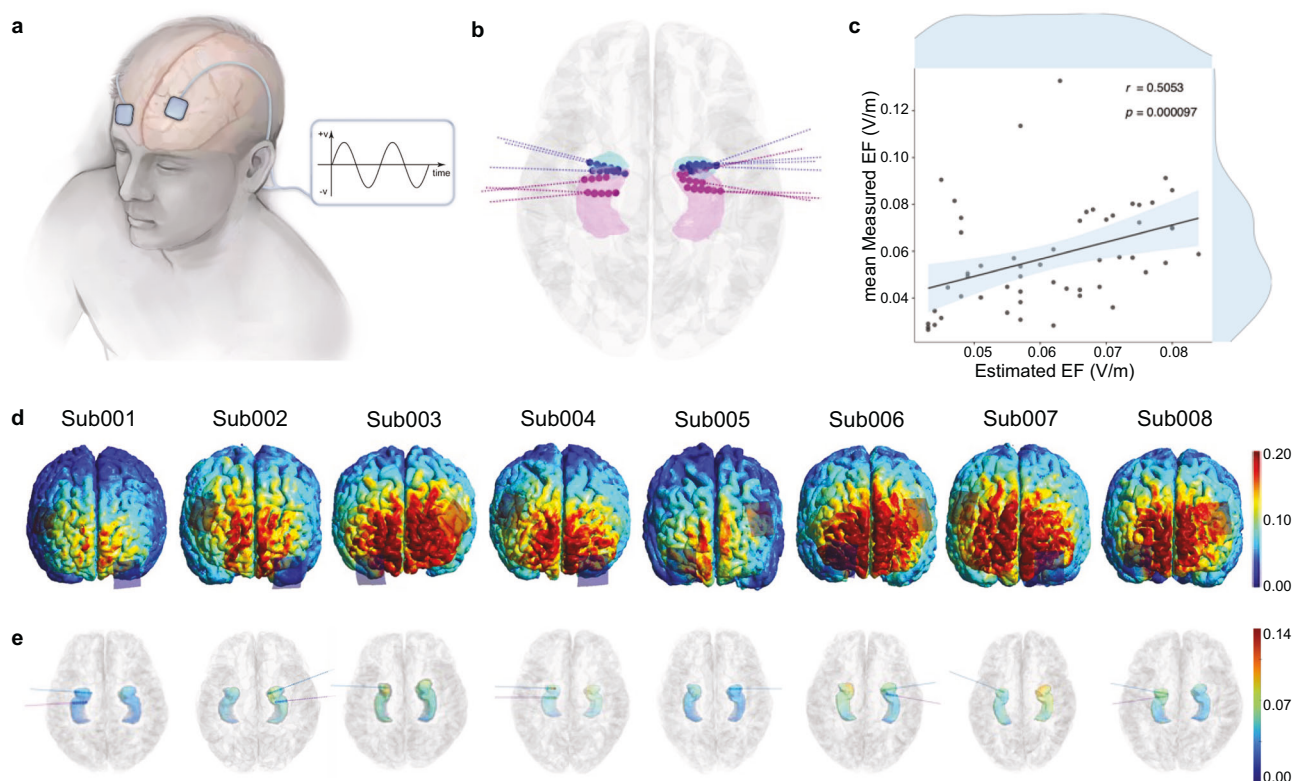


Fig. 1 Experimental setup and electric fields in hippocampus and amygdala. **a** Schematic illustrating transcranial alternating current stimulation (tACS), a non-invasive brain stimulation technique. **b** The implantation sites of the intracranial electrodes rendered onto MNI space. The colored dots indicate the contact in each region, and the differential signal of the two contacts is a channel signal. Blue dots indicate the contacts in the amygdala, and purple dots indicate the contacts in the head of the hippocampus. **c** The correlation between the measured and estimated electric field (EF). **d** The individual EF distribution estimated during peak current at their montages. **e** The individual EF distribution in the hippocampus and amygdala. See also Supplementary Table 1 and Supplementary Fig. 2.

distribution at the current electrode location based on an individual computation model (Fig. 1d), which indicated there may be a direct impact on the subcortical region with 2 mA tACS stimulation (and for Sub001 with 1.5 mA tACS stimulation). Then, we measured the EF magnitudes that reached the hippocampus and amygdala based on the real recordings (Fig. 1b). At 2 mA intensity, we obtained peak EF magnitudes of 0.099 V/m in the hippocampus and 0.147 V/m in the amygdala. The EF magnitudes' mean \pm standard deviation (SD) in these two regions were 0.051 ± 0.022 and 0.062 ± 0.024 V/m, respectively. For each participant, the measured and estimated values of the EF magnitudes in the hippocampus and amygdala were close (as shown in Fig. 1c), there was a similarity between the colors of the electrode contacts and the background color). Moreover, as shown in Fig. 1c, the EF magnitudes showed a good correlation between the measured

and estimated values ($r = 0.505$, $p = 0.000097$); all these values are listed in Supplementary Table 1. Notably, we found that greater stimulation frequency induced the weaker EF magnitudes in the hippocampus and amygdala (Supplementary Fig. 2). These results indicated that non-invasive brain stimulation might reach subcortical regions and have the potential to modulate their neural activity directly.

Modulatory effects of tACS in distinct brain regions

We next compared the LFPs during and after stimulation to baseline (pre-stimulation). The scheme is shown in Fig. 2a. tACS may either facilitate or inhibit the activity level of specific neural oscillations acutely and with lasting effects. We first investigated the different effects of tACS on the hippocampus and amygdala by calculating the power change ratio of each oscillation during-

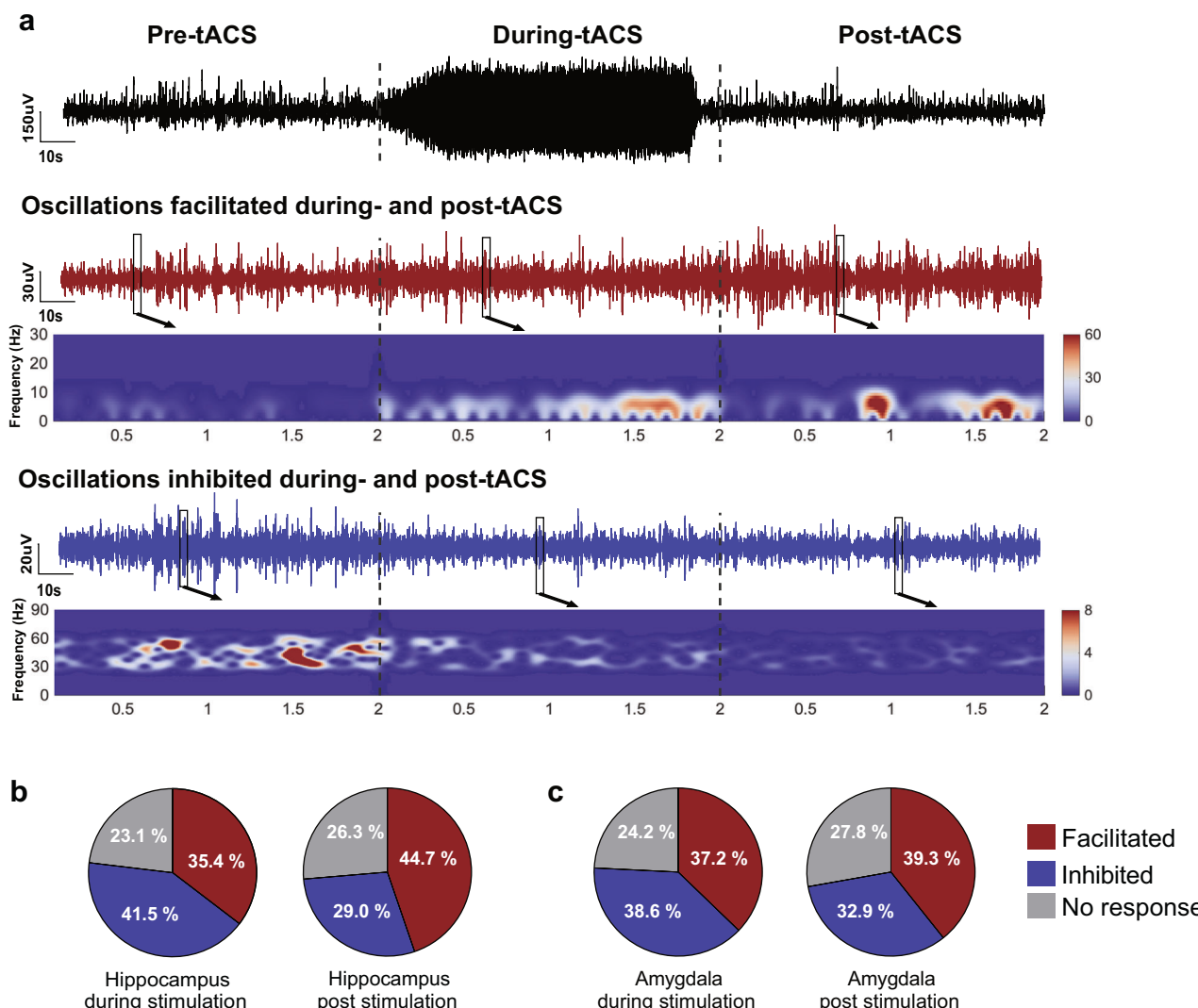


Fig. 2 Characterization of tACS response properties in hippocampus and amygdala. **a**, Illustrations of the power change in neural oscillations during- and post-stimulation compared with the pre-stimulation baseline. **b**, **c**, Lasting effect of tACS responses in the hippocampus and amygdala, which are indexed by the consistency between the relative power change during- and post-stimulation relative to baseline. See also Supplementary Fig. 3.

and post-stimulation compared to pre-stimulation. Then, we divided the neural oscillations according to how they responded to tACS: those that were facilitated (power change ratio > 5%), inhibited (power change ratio < -5%), and had no response (power change ratio within [-5 to 5%]). We combined all the stimulus montages and stimulus frequencies for this analysis to check for overall variation. As shown in Fig. 2b, c, the distribution of the three response types during- and post-stimulation in the hippocampus and amygdala were similar, but the hippocampus showed a more pronounced, lasting effect on the oscillation activity that it facilitated.

In the hippocampus (Fig. 2b), during stimulation 35.4% of oscillations were facilitated, 41.5% inhibited, and 23.1% no response. However, after stimulation, the proportion of facilitated oscillations increased to 44.7% while the inhibition rate decreased to 29.0%, and the no-response rate had a relatively small increase to 26.3%. The chi-square test indicated a significant difference in the distribution of response types between the during- and post-stimulation periods, $\chi^2(2, N=896) = 31.96, p < 0.001$. In the amygdala (Fig. 2c), the proportions during stimulation were 37.2% facilitated, 38.6% inhibited, and 24.2% no response. After stimulation, they became 39.3, 32.9, and 27.8%, respectively. The

chi-square test also indicated a significant difference in the distribution of response types between the during- and post-stimulation periods, $\chi^2(2, N=1400) = 10.45, p = 0.005$. Consistent results were obtained using different thresholds (10, 20, 30, and 40%) to define response types in the hippocampus and amygdala (Supplementary Fig. 3).

The effectiveness of tACS is closely related to the position of the stimulating electrodes. Therefore, we divided the participants into two groups according to the location of the stimulating electrode: one group with the recording electrode ipsilateral to the stimulating electrode placed at F3/F4, and another group with the recording electrode ipsilateral to the stimulating electrode placed at Fp1/Fp2 (Table 2). Then, we performed a statistical test on the effects of different frequencies of tACS on the two groups' hippocampus and amygdala oscillations. For the hippocampus (Fig. 3), when the electrode was ipsilateral to F3/F4, we only observed significant inhibition of high-frequency oscillations including low-gamma, high-gamma, and ultra-frequency band oscillations during 20 Hz tACS (Fig. 3c); when ipsilateral to the Fp1/Fp2, we observed significant facilitation of the theta oscillation during 5 Hz tACS (Fig. 3e) and a wide range of oscillatory changes both during and after 10 Hz tACS (Fig. 3f).

Table 2. Information of recording and signal analysis.

| No. | Montage | tACS Intensity | Recording regions | Number of channels | Analysis groups | Survived epoch rate (%) (Mean ± SD) | | |
|--------|---------|----------------|-------------------|--------------------|------------------------|-------------------------------------|-------------|-------------|
| | | | | | | Pre | During | Post |
| Sub001 | F4-FP1 | 1.5 mA | L Amygdala | 5 | Ipsilateral to FP1/FP2 | 73.3 ± 8.5 | 93.8 ± 2.8 | 72.7 ± 13.5 |
| | | | L Hippocampus | 4 | | | | |
| Sub002 | F4-FP1 | 2 mA | R Amygdala | 4 | Ipsilateral to F3/F4 | 54.4 ± 8.8 | 68.4 ± 17.0 | 55.8 ± 8.6 |
| | | | R Hippocampus | 3 | | | | |
| Sub003 | F3-FP2 | 2 mA | L Amygdala | 2 | Ipsilateral to F3/F4 | 90.8 ± 4.1 | 96.6 ± 3.0 | 89.4 ± 3.2 |
| | | | L Hippocampus | 3 | | | | |
| Sub004 | F4-FP1 | 2 mA | L Amygdala | 2 | Ipsilateral to FP1/FP2 | 67.5 ± 7.0 | 77.2 ± 7.4 | 71.0 ± 10.4 |
| | | | L Hippocampus | 3 | | | | |
| Sub005 | F3-FP2 | 2 mA | R Amygdala | 3 | Ipsilateral to FP1/FP2 | 38.3 ± 6.3 | 51.3 ± 24.1 | 40.4 ± 9.5 |
| | | | R Hippocampus | 3 | | | | |
| Sub006 | F3-FP2 | 2 mA | R Amygdala | 4 | Ipsilateral to FP1/FP2 | 67.7 ± 12.3 | 74.3 ± 12.7 | 61.2 ± 12.8 |
| | | | R Hippocampus | 3 | | | | |
| Sub007 | F4-FP1 | 2 mA | L Amygdala | 1 | Ipsilateral to FP1/FP2 | 88.3 ± 3.1 | 96.6 ± 2.1 | 93.8 ± 3.2 |
| | | | L Hippocampus | 3 | | | | |
| Sub008 | F3-FP2 | 2 mA | L Amygdala | 4 | Ipsilateral to F3/F4 | 49.7 ± 8.8 | 60.8 ± 8.0 | 55.2 ± 9.8 |
| | | | L Hippocampus | 3 | | | | |

All results pertaining to the hippocampus are summarized in Fig. 3i.

For the amygdala (Fig. 4), whether ipsilateral to F3/F4 or Fp1/Fp2, the significant changes always occurred sporadically, and in response to both 10 and 40 Hz tACS. When ipsilateral to F3/F4, the theta, high-gamma, and ultra-frequency band oscillations during 10 Hz tACS (Fig. 4b) and the beta and ultra-frequency band oscillations during 40 Hz tACS (Fig. 4d) were both inhibited. When ipsilateral to the Fp1/Fp2, only alpha oscillation during 10 Hz tACS (Fig. 4f) and the low-gamma and ultra-frequency band oscillations after 40 Hz tACS (Fig. 4h) were facilitated. All results pertaining to the amygdala are summarized in Fig. 4i.

These results indicated that the neural oscillations in the hippocampus respond strongly and stably to 10 Hz stimulation, specifically when the recording electrodes were ipsilateral to Fp1/Fp2. Furthermore, we investigated the potential after-effects of the transient tACS procedure. When directly comparing the effects of during- and post-stimulation, we only observed consistently significant changes in the hippocampus (Fig. 3i), not in the amygdala (Fig. 4i). For example, oscillations underwent significant changes during 10 Hz tACS and further intensified after the stimulation in the hippocampus but tended to weaken after the stimulation in the amygdala (Supplementary Fig. 4). The observed discrepancy between the response of the hippocampus and amygdala aligns with the results presented in Fig. 2b, c, and it can be attributed to the hippocampus exhibiting a more consistent response to 10 Hz stimulation.

State-dependent effects of tACS

We further examined whether the power change ratios of neural oscillations during- or post-stimulation were associated with their innate activity level pre-stimulation, i.e., state-dependent responses. In the hippocampus, significant relationships were only found between power change ratios after 10 Hz tACS and the corresponding oscillation activity level pre-stimulation (Fig. 5a). The four types of oscillation for which we found significant relationships were ultra-frequency ($r = -0.601$, $p = 0.003$), beta ($r = -0.568$, $p = 0.003$), high-gamma ($r = -0.501$, $p = 0.007$), and alpha ($r = -0.500$, $p = 0.006$) (Fig. 5c–f). These state-dependent responses were consistent with the broad response during and after 10 Hz tACS. At 5, 20, and 40 Hz tACS, no state-dependent responses were found for any type of oscillation.

For the amygdala, we observed broad state-dependent responses during and after 10, 20, and 40 Hz tACS (Fig. 5b). The significant correlation coefficients ranged from -0.653 to -0.353 . The four oscillations with the strongest correlations were alpha during 20 Hz tACS ($r = -0.653$), low-gamma during 40 Hz tACS ($r = -0.619$), alpha after 10 Hz tACS ($r = -0.570$) and beta after 10 Hz tACS ($r = -0.527$) (Fig. 5g–j, all $p < 0.001$). However, most of these state-dependent responses did not persistently follow the stimulation, which might potentially be due to the short stimulation period. Complete information on the relationships between the effects of tACS on neural oscillations and the pre-stimulus level of oscillation can be found in Supplementary Figs. 5 and 6.

DISCUSSION

In summary, here we present evidence in the live human brain that 10 Hz tACS may induce the most pronounced effect on neural oscillations, especially in the hippocampus. These findings not only validate that the current of a generalized tACS protocol can reach human deep brain regions, but also establish that it can modulate the activity of their neural oscillations, which may be the key to the ability of tACS to improve cognitive function and ameliorate disease states [19]. The oscillatory changes we observed in the hippocampus and amygdala can be summarized in two response patterns: 1) low- and high-frequency neural oscillations appeared to behave distinctly in response to stimulation, and 2) oscillations were more responsive to tACS when the recording site was near the mPFC (Fp1/Fp2). Furthermore, we found that neural oscillations showed a wide range of state-dependent responses to tACS and in its aftermath. When the baseline activity of the brain was stronger, the response to tACS was weaker, which suggests that a stronger stimulation current may be required. Notably, we identified the rather specific effects of 10 Hz tACS on the hippocampus, which warrant future investigations related to the behavioral changes this effect could induce.

Potential mechanisms of 10 Hz tACS-specific modulation of hippocampal neural activity

Previous studies have shown that the EF intensity is key to successfully modulating brain function [31]. Studies in mice and non-human primates suggest that 0.3 V/m EF may be the

SEEG recordings in hippocampus

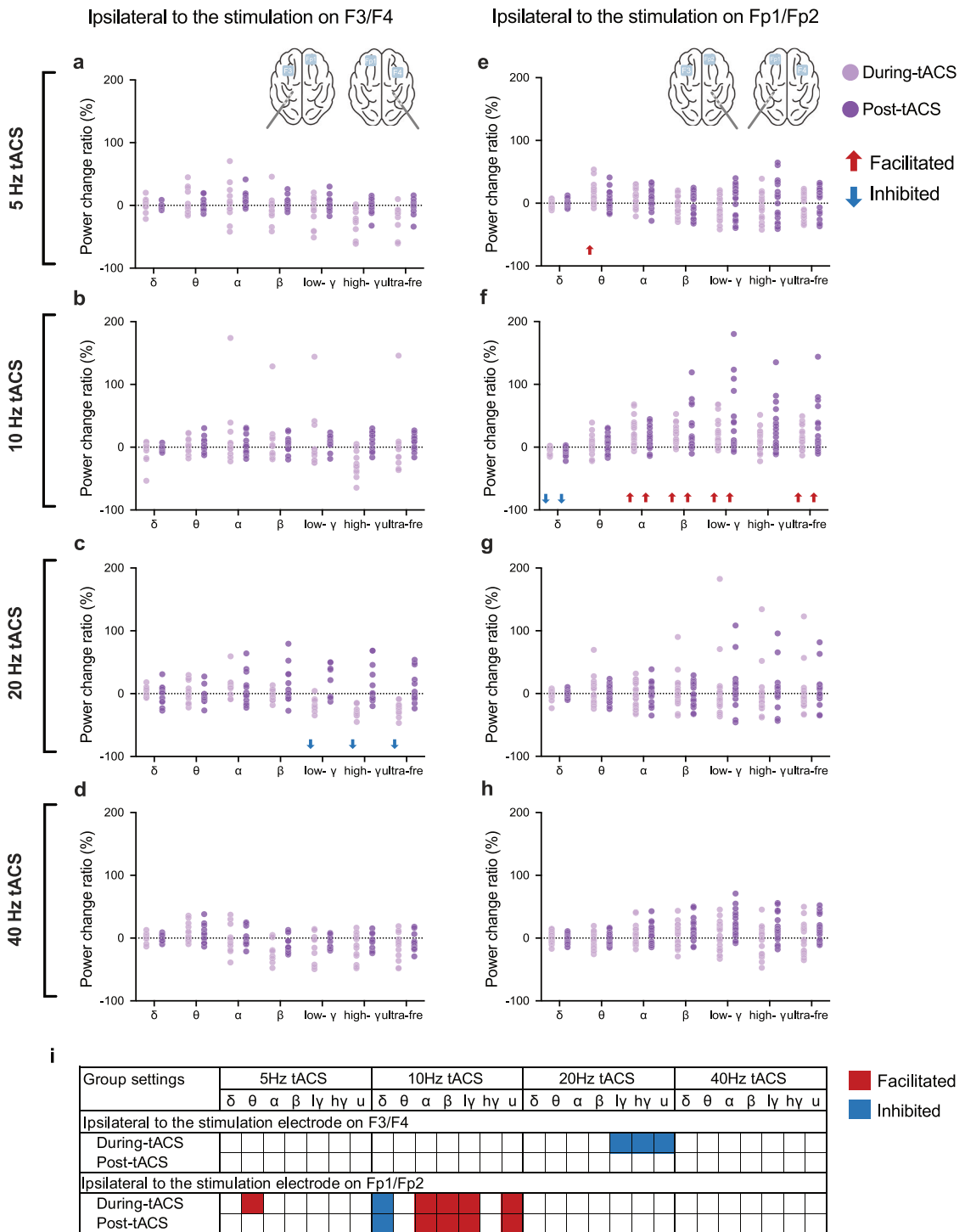


Fig. 3 Relative power change of the neural oscillations in the hippocampus during- and post-stimulation with tACS at different stimulation frequencies. Results are grouped by the relative position between the recording and stimulation electrodes and shown in **a–d**, ipsilateral to F3/F4, and **e–h**, ipsilateral to Fp1/Fp2, respectively. Each dot represents one channel of bipolar recording and there were 16 channels in total. **i** Summary of the significance and direction of the oscillation changes. The statistical significance level was set at 0.01 and corrected for multiple comparisons using the FDR correction. It can be seen that the neural oscillations in the hippocampus responded mainly to 10 Hz tACS and they were consistent between the during-stimulation and post-stimulation periods. See also Supplementary Fig. 4a.

minimum effective dose for tACS [20]. The present study found that EFs reaching the hippocampus and amygdala were in the range of 0.03–0.1 V/m. These values are lower than those reported in a previous study, when stimulation electrodes were placed on

the temporal lobe (i.e., FT9-FT10 or T7-C4 or C3-FT10 montages), which found the mean and SD of EF under 1 mA stimulation were 0.17 ± 0.06 and 0.21 ± 0.08 V/m [32]. On the other hand, our values are higher than those found when stimulation electrodes were

SEEG recordings in amygdala

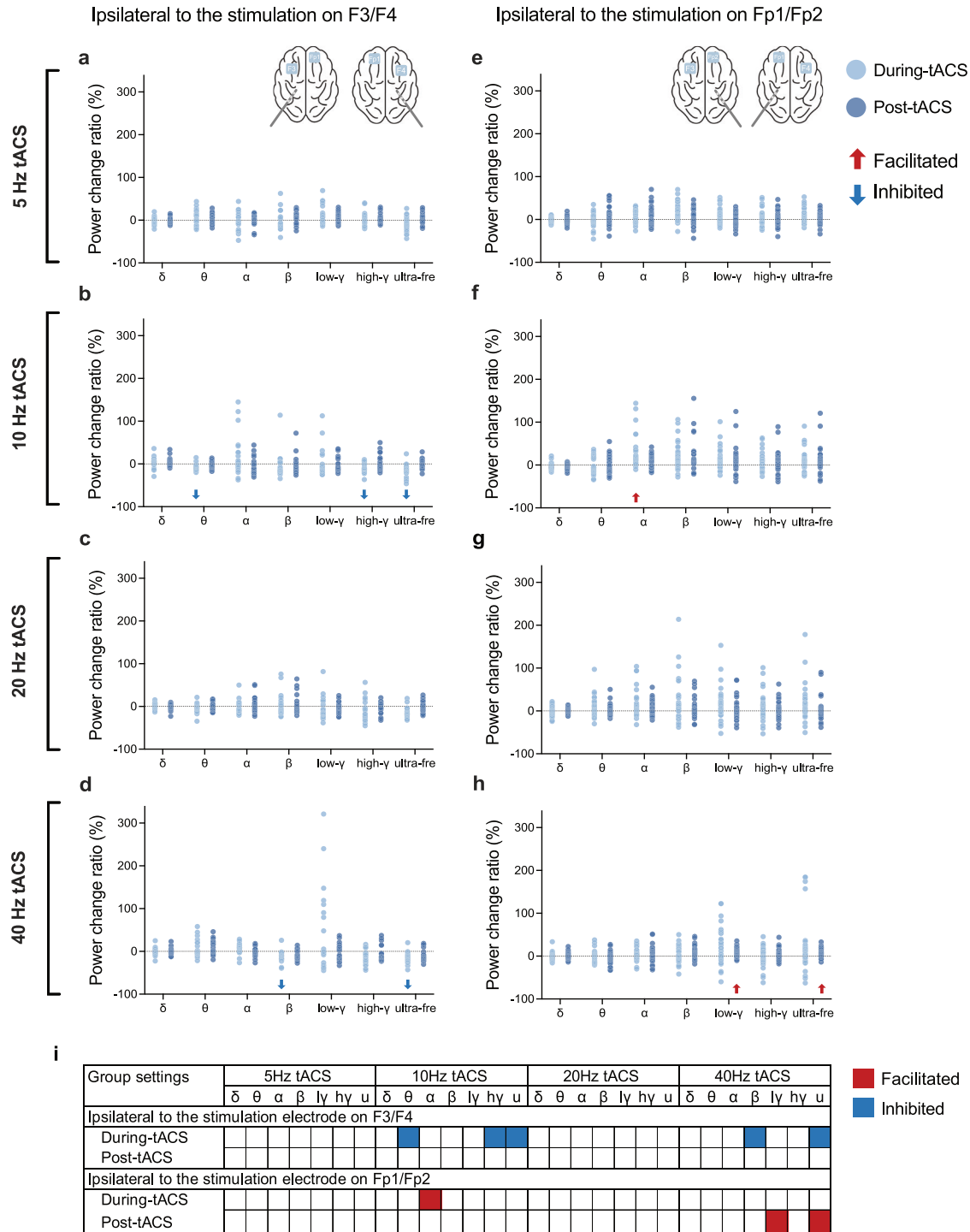


Fig. 4 Relative power change of the neural oscillations in the amygdala during- and post-stimulation with tACS at different stimulation frequencies. Results are grouped by the relative position between the recording and stimulation electrodes and shown in **a-d**, ipsilateral to the F3/F4, and **e-h**, ipsilateral to Fp1/Fp2, respectively. Each dot represents one channel of bipolar recording and there were 25 channels in total. **i** Summary of the significance and direction of the oscillation changes. The statistical significance level was set at 0.01 and corrected for multiple comparisons using the FDR correction. It can be seen that the neural oscillations in the amygdala responded in a dispersed manner and were not consistent between the during- and post-stimulation periods. See also Supplementary Fig. 4b.

placed on the frontal and central lobe (i.e., Fz-C3 or Fz-C4), for which the mean and SD of EF under 1 mA stimulation measured in the amygdala were around 0.05–0.08 V/m [32]. The results of all studies illustrate that the strength of the EF reaching the

hippocampus and amygdala is closely dependent on the proximity of the stimulating electrode, and viewed in this larger context of the literature, we find that our results are within a reasonable range.

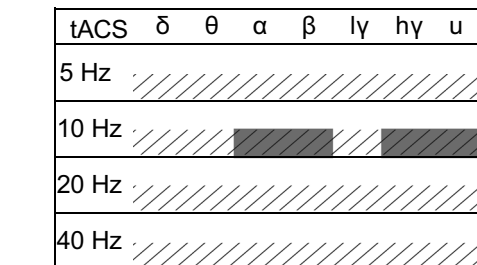
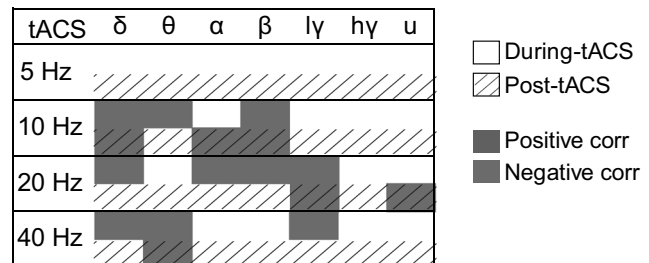
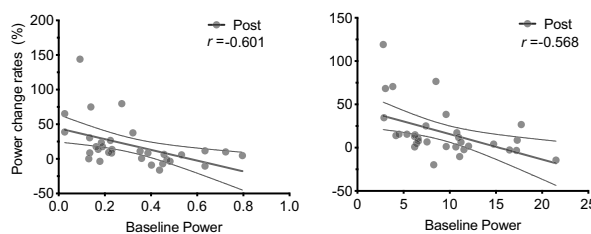
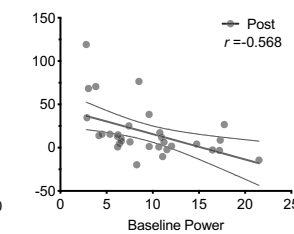
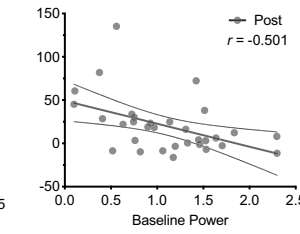
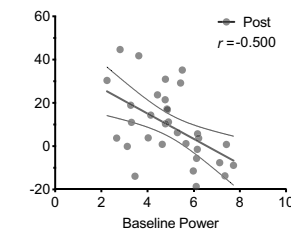
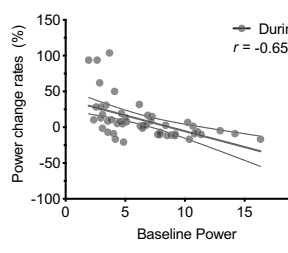
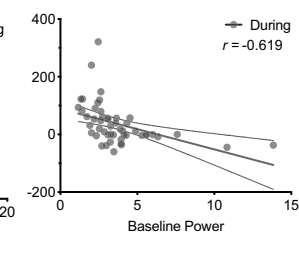
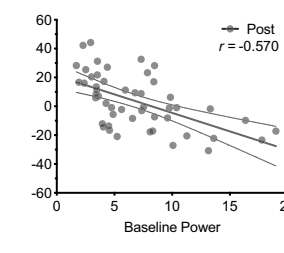
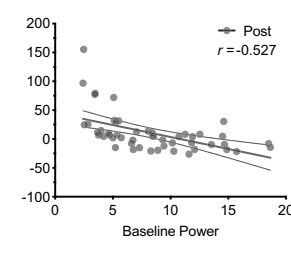
a State dependence effect in hippocampus

b State dependence effect in amygdala
**c** ultra oscillation changes after 10Hz tACS**d** β oscillation changes after 10Hz tACS**e** high γ oscillation changes after 10Hz tACS**f** α oscillation changes after 10Hz tACS**g** α oscillation changes during 20Hz tACS**h** low γ oscillation changes during 40Hz tACS**i** α oscillation changes after 10Hz tACS**j** β oscillation changes after 10Hz tACS

Fig. 5 State-dependence of the neural responses to tACS in the hippocampus and amygdala. a, b Summary of the significance and direction of the state-dependent effect. See also Supplementary Figs. 5–6. The four scatter plots with the most significant absolute values of the correlation coefficients in **c–f** for the hippocampus and **g–j** for the amygdala are listed in descending order. The level of statistical significance was set at 0.01 and corrected for multiple comparisons using the FDR correction. In **a** and **b**, the green color means remarkable negative relationship and the red color means remarkable positive relationship, the significant level was $p < 0.01$. The state-dependent response in the hippocampus was largely consistent with its broad response to 10 Hz tACS, especially after tACS. The amygdala showed a wide range of state-dependent responses, but most neural oscillations did not significantly change during- or post-stimulation.

The present study showed that 10 Hz mPFC tACS was able to effectively modulate neural oscillatory activities in the hippocampus even with such a low EF. Therefore, to verify whether this was a direct effect of the tACS, we calculated the correlation between the EF intensity induced by F3/F4 or Fp1/Fp2 tACS and the power change rate in the hippocampus and amygdala during- and post-stimulation. As shown in Supplementary Fig. 8, for mPFC stimulation, only the EF intensity of 5 Hz tACS was significantly correlated with the power change of oscillations during stimulation in the hippocampus, whereas 10 Hz tACS was significantly correlated with the power change of oscillations post-stimulation. For DLPFC stimulation, only the EF intensity of 40 Hz tACS was significantly correlated with the power change of oscillations during stimulation in the hippocampus. However, no significant relationship was found between changes in neural activity in the amygdala and EF intensity. These results suggest that tACS has the potential to directly modulate hippocampal function even with only relatively weak electrical stimulation conducted from the scalp. But at the same time, these results also prove that the phenomena we reported in this study largely cannot be explained by the direct effect of EF.

The neural response observed in the hippocampus may also result from large-scale network-level interactions between many brain regions, as neuroimaging studies have reported that the connectivity of the default mode network, in which mPFC acts as a critical region, may be specifically enhanced by 10 Hz tACS

[33, 34]. A Transcranial Magnetic Stimulation (TMS) intervention study further suggested that the mPFC-hippocampal network plays an important role in neuromodulation for treating psychiatric disorders [24]. The same study found that DLPFC TMS ameliorated depression based on effective modulation of hippocampal function, and that this improvement was mediated by the mPFC. Consistent with our results, the results of this study also indicated that the mPFC may be a better target for treating depression [35]. We analyzed the electrodes inserted into the mPFC (23 channels of bipolar recordings from 28 contacts) and found that there was a significant response to tACS at all frequencies in the mPFC, with the most persistent stimulatory effect using 40 Hz tACS, and this response extended beyond the end of the stimulation (Supplementary Fig. 7). These results suggest that a network containing the mPFC and the hippocampus may work like a frequency filter, delivering information of a specific frequency (10 Hz) to the hippocampus.

The potential mechanisms of state-dependent tACS effects

The state-dependent neural response observed in the hippocampus was largely consistent with its broad response to 10 Hz tACS, especially post-stimulation. In contrast, the state-dependent responses observed in the amygdala differed from its frequency response, occurring in a dispersed manner and showing extensive state-dependent alterations. These differences between the hippocampus and amygdala may be due to their responses to

the current stimulus pattern. For the hippocampus, the modulatory effect is predictably influenced by its current state, since 10 Hz tACS at Fp1/Fp2 can significantly modulate neural oscillatory activity in the hippocampus. The state-dependent effects observed in the hippocampus can be explained by the fact that the modulation of brain regions by exogenous physical fields (EFs or oscillations from other regions) is influenced by their endogenous level of neural activity. And the effect is manifested only if the exogenous physical field can successfully modulate otherwise it is submerged in the autonomic activity of the target region. Whereas the endogenous activity of the amygdala is more influenced by its own level of activity as the current tACS protocol can not effectively regulate its activity, thus showing a broader state dependence.

Limitations

There are several limitations to this study. First, our participants were epileptic patients, and the number of participants was relatively small. We made many efforts to maximize the possibility of extending our findings to a broader population by ensuring that participants were not taking medication, excluding data recorded from an epileptic focus, and removing the epochs with epileptiform discharges. Second, because the participants experienced skin sensations, as is normally reported with tACS, it cannot be ruled out that neural oscillations may be influenced by individual attention and/or changes in feelings brought about by these sensations. However, since the participants experienced skin sensations at each stimulation frequency, this could not explain the frequency-specific phenomenon of stable neural oscillation changes observed only with 10 Hz stimulation. Third, the results of the present study only highlight that prefrontal tACS can affect neural oscillations in the hippocampus, while the mechanism underlying this phenomenon still needs to be resolved by collecting data from more patients and recording more locations. Furthermore, a lack of single-neuron activity recording limits our interpretation of the mechanism. Last but not least, future investigations should probe the effects of longer tACS protocols (e.g., 20 min), which are more clinically relevant in treating neurological and psychiatric patients.

In conclusion, here we establish frequency-tuned and state-dependent neural responses as intracranial physiological mechanisms induced by non-invasive brain stimulation. The findings may inspire the innovation and optimization of brain stimulation therapy for neurological and psychiatric diseases.

DATA AVAILABILITY

The data that support the findings of this study are openly available at the Open Science Foundation repository (<https://doi.org/10.17605/OSF.IO/G9BCT>).

REFERENCES

- Polania R, Nitsche MA, Ruff CC. Studying and modifying brain function with non-invasive brain stimulation. *Nat Neurosci*. 2018;21:174–87.
- Grover S, Nguyen JA, Reinhart RMG. Synchronizing brain rhythms to improve cognition. *Annu Rev Med*. 2021;72:29–43.
- Krause MR, Vieira PG, Csorba BA, Pilly PK, Pack CC. Transcranial alternating current stimulation entrains single-neuron activity in the primate brain. *Proc Natl Acad Sci USA*. 2019;116:5747–55.
- Axmacher N, Henseler MM, Jensen O, Weinreich I, Elger CE, Fell J. Cross-frequency coupling supports multi-item working memory in the human hippocampus. *Proc Natl Acad Sci USA*. 2010;107:3228–33.
- Grover S, Wen W, Viswanathan V, Gill CT, Reinhart RMG. Long-lasting, dissociable improvements in working memory and long-term memory in older adults with repetitive neuromodulation. *Nat Neurosci*. 2022;25:1237–46.
- Zhou D, Li A, Li X, Zhuang W, Liang Y, Zheng C-Y, et al. Effects of 40 Hz transcranial alternating current stimulation (tACS) on cognitive functions of patients with Alzheimer's disease: a randomised, double-blind, sham-controlled clinical trial. *J Neurol Neurosurg Psychiatry*. 2022;93:568–70.
- Benussi A, Cantoni V, Grassi M, Brechet L, Michel CM, Datta A, et al. Increasing brain gamma activity improves episodic memory and restores cholinergic dysfunction in Alzheimer's disease. *Annu Neurol*. 2022;92:322–34.
- Simons JS, Ritchey M, Fernyhough C. Brain mechanisms underlying the subjective experience of remembering. *Annu Rev Psychol*. 2022;73:159–86.
- Tavakoli AV, Yun K. Transcranial alternating current stimulation (tACS) mechanisms and protocols. *Front Cell Neurosci*. 2017;11:214.
- Underwood E. Cadaver study challenges brain stimulation methods. *Science*. 2016;352:397.
- Opitz A, Falchier A, Linn GS, Milham MP, Schroeder CE. Limitations of ex vivo measurements for in vivo neuroscience. *Proc Natl Acad Sci*. 2017;114:5243–6.
- Gallen CL, D'Esposito M. Brain modularity: a biomarker of intervention-related plasticity. *Trends Cognit Sci*. 2019;23:293–304.
- Johnson L, Alekseichuk I, Krieg J, Doyle A, Yu Y, Vitek J, et al. Dose-dependent effects of transcranial alternating current stimulation on spike timing in awake nonhuman primates. *Sci Adv*. 2020;6:eaaz2747.
- Huang WA, Stitt IM, Negahbani E, Passey DJ, Ahn S, Davey M, et al. Transcranial alternating current stimulation entrains alpha oscillations by preferential phase synchronization of fast-spiking cortical neurons to stimulation waveform. *Nat Commun*. 2021;12:3151.
- Helfrich RF, Schneider TR, Rach S, Trautmann-Lengsfeld SA, Engel AK, Herrmann CS. Entrainment of brain oscillations by transcranial alternating current stimulation. *Curr Biol*. 2014;24:333–9.
- Kurmann R, Gast H, Schindler K, Fröhlich F. Rational design of transcranial alternating current stimulation: identification, engagement, and validation of network oscillations as treatment targets. *Clin Transl Neurosci*. 2018;2:33. 2514183x18793515.
- Bradley C, Nydam AS, Dux PE, Mattingley JB. State-dependent effects of neural stimulation on brain function and cognition. *Nat Rev Neurosci*. 2022;23:459–75.
- Lafon B, Henin S, Huang Y, Friedman D, Melloni L, Thesen T, et al. Low frequency transcranial electrical stimulation does not entrain sleep rhythms measured by human intracranial recordings. *Nat Commun*. 2017;8:1199.
- Lee TL, Lee H, Kang N. A meta-analysis showing improved cognitive performance in healthy young adults with transcranial alternating current stimulation. *npj Sci Learn*. 2023;8:1.
- Wischniewski M, Alekseichuk I, Opitz A. Neurocognitive, physiological, and biophysical effects of transcranial alternating current stimulation. *Trends Cognit Sci*. 2023;27:189–205.
- Chen S, Tan Z, Xia W, Gomes CA, Zhang X, Zhou W, et al. Theta oscillations synchronize human medial prefrontal cortex and amygdala during fear learning. *Sci Adv*. 2021;7:eabf4198.
- Zheng J, Stevenson RF, Mander BA, Mnatsakanyan L, Hsu FPK, Vadera S, et al. Multiplexing of theta and alpha rhythms in the amygdala-hippocampal circuit supports pattern separation of emotional information. *Neuron*. 2019;102:887–98.
- Pacheco Estefan D, Sánchez-Fibla M, Duff A, Principe A, Rocamora R, Zhang H, et al. Coordinated representational reinstatement in the human hippocampus and lateral temporal cortex during episodic memory retrieval. *Nat Commun*. 2019;10:2255.
- Han S, Li XX, Wei S, Zhao D, Ding J, Xu Y, et al. Orbitofrontal cortex-hippocampus potentiation mediates relief for depression: a randomized double-blind trial and TMS-EEG study. *Cell Rep Med*. 2023;4:101060.
- Fischl B, Salat DH, Busa E, Albert M, Dieterich M, Haselgrove C, et al. Whole brain segmentation: automated labeling of neuroanatomical structures in the human brain. *Neuron*. 2002;33:341–55.
- Brunyé TT, Beaudoin ME, Feltman KA, Heaton KJ, McKinley RA, Vartanian O, et al. Neuroenhancement in military personnel: conceptual and methodological promises and challenges. In: *NATO Symposium on Applying Neuroscience to Performance: From Rehabilitation to Human Cognitive 2021*, Rome, Italy, 11–12 October 2021. 2022.
- Higgins N, Forlini C, Butorac I, Gardner J, Carter A. Anticipating the future of neurotechnological enhancement. In: *The Routledge Handbook of the Ethics of Human Enhancement*. New York, NY, USA: Routledge. 2024. p. 237–50.
- Illes J, Hossain S. Neuroethics: anticipating the future. New York, NY, USA: Oxford University Press; 2017.
- Thielscher A, Antunes A, Saturnino GB. Field modeling for transcranial magnetic stimulation: a useful tool to understand the physiological effects of TMS? In: *2015 37th Annual International Conference of the IEEE Engineering in Medicine and Biology Society (EMBC)*. Milan, Italy: IEEE; 2015. p. 222–5.
- Puonti O, Van Leemput K, Saturnino GB, Siebner HR, Madsen KH, Thielscher A. Accurate and robust whole-head segmentation from magnetic resonance images for individualized head modeling. *NeuroImage*. 2020;219:117044.

31. Shan Y, Wang H, Yang Y, Wang J, Zhao W, Huang Y, et al. Evidence of a large current of transcranial alternating current stimulation directly to deep brain regions. *Mol Psychiatry*. 2023;28:5402–10.
32. Louvion S, Tyvaert L, Maillard LG, Colnat-Coulbois S, Dmochowski J, Koessler L. Transcranial electrical stimulation generates electric fields in deep human brain structures. *Brain Stimulation*. 2022;15:1–12.
33. Weinrich CA, Brittain JS, Nowak M, Salimi-Khorshidi R, Brown P, Stagg CJ. Modulation of long-range connectivity patterns via frequency-specific stimulation of human cortex. *Curr Biol*. 2017;27:3061–3068.e3.
34. Clancy KJ, Andrzejewski JA, You Y, Rosenberg JT, Ding M, Li W. Transcranial stimulation of alpha oscillations up-regulates the default mode network. *Proc Natl Acad Sci USA*. 2022;119:e2110868119.
35. Scangos KW, Makhoul GS, Sugrue LP, Chang EF, Krystal AD. State-dependent responses to intracranial brain stimulation in a patient with depression. *Nat Med*. 2021;27:229–31.

ACKNOWLEDGEMENTS

The authors would like to acknowledge Professor Jian Jiang of Lingang Laboratory for supporting technical to help test the robust of tACS equipment, Hui Zheng for his great help in visualization and all volunteers for participating in this study.

AUTHOR CONTRIBUTIONS

Conceptualization: Ti-Fei Yuan, Jiwen Xu, Quanying Liu. Funding acquisition: Ti-Fei Yuan, Quanying Liu, Pengfei Wei, Huichun Luo. Data collection: Huichun Luo, Xiaolai Ye, Hui-Ting Cai, Qiangqiang Liu, Ying Xu, Ziyu Mao, Yanqing Cai, Jing Hong. Methodology: Huichun Luo, Xiaolai Ye, Hui-Ting Cai, Mo Wang. Writing - original draft: Huichun Luo, Xiaolai Ye, Hui-Ting Cai, Mo Wang, Yue Wang, Chencheng Zhang. Writing - review & editing: Huichun Luo, Hui-Ting Cai, Pengfei Wei, Yong Lu, Quanying Liu, Jiwen Xu, Ti-Fei Yuan.

FUNDING

This work was supported by the National Natural Science Foundation of China (T2394535, T2394533, 82325019, 32241015, 82401432), the Shanghai Yangfan Program (21YF1439700), the Science and Technology Commission of Shanghai Municipality (23XD1423000, 23ZR1480800, 24ZR1461000), Shanghai Municipal Commission of Health (2022JC016), Shanghai Municipal Education Commission - Gaofeng Clinical Medicine Grant Support (20181715), and Excellent Young Scientists Fund in Shenzhen (RCYX20231211090405003).

COMPETING INTERESTS

The authors declare no competing interests.

ADDITIONAL INFORMATION

Supplementary information The online version contains supplementary material available at <https://doi.org/10.1038/s41380-025-02892-7>.

Correspondence and requests for materials should be addressed to Quanying Liu, Jiwen Xu or Ti-Fei Yuan.

Reprints and permission information is available at <http://www.nature.com/reprints>

Publisher's note Springer Nature remains neutral with regard to jurisdictional claims in published maps and institutional affiliations.

Springer Nature or its licensor (e.g. a society or other partner) holds exclusive rights to this article under a publishing agreement with the author(s) or other rightsholder(s); author self-archiving of the accepted manuscript version of this article is solely governed by the terms of such publishing agreement and applicable law.